Available online at www.sciencedirect.com
ScienceDirect
Lithos 96 (2007) 22–35
LITHOS
www.elsevier.com/locate/lithos

A possible model for the lithospheric thinning of North China Craton: Evidence from the Yanshanian (Jura-Cretaceous) magmatism and tectonism

Jinfu Deng [a,*], Shangguo Su [a], Yaoling Niu [a,b], Cui Liu [a], Guochun Zhao [a], Xingguo Zhao [a], Su Zhou [a], Zongxu Wu [a]

[a] *State Key Laboratory of Geological processes and Mineral Resources, School of Earth and Resources Sciences, Key Laboratory of Lithosphere Tectonics and Lithoprobing Technology of Ministry of Education, China University of Geosciences, Beijing 100083, China*
[b] *Department of Earth Sciences, Durham University, Durham DH1 3LE,UK*

Received 22 February 2006; accepted 5 September 2006
Available online 8 January 2007

Abstract

It is well known that the North China Craton was largely formed in the Archean, and was reactivated and transformed during the Jura-Cretaceous (Yanshanian) time into an orogenic belt, which is believed to be related to the lithospheric thinning. Recent debate is centered on the mechanisms and processes of the lithospheric thinning. There are two prevailing models for the lithosphere thinning: (1) thermal erosion or/and chemical metasomatism allowed the lower part of the lithospheric mantle to be transformed into asthenosphere, (2) delamination of the lithospheric mantle, and perhaps also the lowermost crust.

In this paper, we attempt to explain how the buoyant cratonic lithosphere may be transformed into a denser one, allowing delamination to take place on the basis of field observation, tectonic analysis and petrologic data on igneous rocks formed during the Yanshanian. We recognize four episodes of contractional deformation that resulted in significant crustal shortening and vertical thickening. The counter-clockwise Pressure–Temperature–time path of the tectonomagmatic events suggests that the underplating basaltic magma may have heated and weakened the existing cold and strong crust. This crustal change in rheology may have facilitated the contractional deformation and crustal thickening. Petrologic data of the contemporary igneous rocks and the lower crustal xenoliths suggest that the crust had reached ~50–65 km in thickness. It suggests that input of large amount of asthenosphere-derived mafic magmas is required to cause crustal melting. Thus, a large amount of eclogite may be formed at the lowermost crust following the transient thickening events. The dense eclogite may trigger the lithosphere delamination.

Keywords: North China Craton; Yanshanian orogenic belt; Magmatism and tectonic deformation; Delamination and lithospheric thinning

1. Introduction

It is well known that the North China Craton was largely formed in the Archean, and was reactivated and transformed during the Jura-Cretaceous (Yanshanian) time into an orogenic belt. The latter is believed to be

* Corresponding author. Tel.: +86 10 62009527; fax: +86 10 82321115.
E-mail addresses: dengjf@cugb.edu.cn, dengjinfu@21cn.com (J. Deng).

0024-4937/$ - see front matter © 2006 Elsevier B.V. All rights reserved.
doi:10.1016/j.lithos.2006.09.009

related to the lithospheric thinning from the ~200–250 km cratonic lithospheric root to the present-day thickness of about 60–70 km (e.g. Zhang et al., 1983; Liu, 1987; Deng, 1988; Menzies et al., 1993; Deng et al., 1994, 2004c).

The main question is what mechanisms during the Jura-Cretaceous time may have actually caused the lithospheric thinning of the buoyant continental root (or keel) which is generally believed to be tectonically stable. There are two prevailing models: (1) Basal thermal erosion and chemical metasomatism are considered to cause the lower part of the lithospheric mantle to be transformed into asthenosphere (e.g. Menzies and Xu, 1998; Griffin et al., 1998; Xu, 2001; Zhou et al., 2002; Zhang et al., 2002, 2003; Chen et al., 2003) in response to some mantle thermal events, which emphasizes the importance of the lithospheric rheology change relative to possible/probable density variation. However, Niu (2005) considers "thermal erosion" is unlikely because of lacking excess heat source, but advocates that the base of the old lithospheric mantle had been transformed into the convective asthenosphere (rheology change) by hydration-weakening, for which the required water or hydrous melt may come from dehydration of the subducted Paleo-Pacific lithosphere that lies horizontally in the transition zone beneath eastern China. (2) Delamination of the lower part of the lithospheric mantle or the entire lithospheric mantle including the lowermost crust (e.g. Gao et al., 1992; Deng et al., 1994, 1996; Gao et al., 1998; Wu et al., 2000, 2002; Zheng et al., 2003; Deng et al., 2003, 2004a; Gao et al., 2004), which stress the importance of lithospheric density (vs. rheology) change.

In this paper, we present a model that attempted to explain what may have caused the buoyant lithosphere of North China Craton to become denser so that the dense portion may sink into the asthenospheric mantle by a process commonly termed "delamination." This model is based on analysis of tectonic deformation during the Yanshanian (Jura-Cretaceous) time, the petrology of the contemporary igneous rocks and thermal consideration.

2. Sequence of tectonomagmatic events in the Yanshan orogenic belt of North China during Jura-Cretaceous time and tectonic thickening of the crust

2.1. Yanshanian orogenesis

The term "Yanshanian orogenesis" was first proposed in 1927 by Wong (1927) based mainly on the geological survey in Beijing area, eastern Hebei province and western Liaoning province, to describe the orogenesis during Jura-Cretaceous time characterized by intensive magmatism and tectonic deformation as well as mineralization. Fig. 1 is a simplified map showing the distribution of volcanic rocks, and Fig. 2 is for intrusive rocks in the Yanshan belt. Much research on the Yanshanian orogenesis has been done over the years. The current consensus is that associated with the Yanshan orogenesis is the inferred lithosphere thinning beneath eastern China, especially beneath the North China Craton.

Current debate primarily focuses on what mechanisms and processes may have actually caused such lithospheric thinning, and whether there was any crustal thickening associated with the lithospheric thickening during the Jura-Cretaceous (Yanshanian) time.

There are several open questions on the crustal thickening. (1) How can contractional tectonic deformation develop in the cold and strong cratonic crust? (2) Some researchers (e.g. Menzies and Xu, 1998; Griffin et al., 1998; Chen et al., 2002, 2005; Ge et al., 2002) do not consider the possibility of crustal thickening because of the development of extensional basins. (3) Others believe that crustal thickening indeed occurred as a result of tectonic thickening (e.g. Deng et al., 1996; Davis, 2003; Zhang et al., 2003) or basaltic magma underplating (e.g. Xu et al., 2004). (4) There is a further debate, among those who accept crustal thickening, on the timing of tectonic transition from contractional deformation to extensional deformation. One model suggests the Late Jurassic (J_3) (e.g. Lu et al., 1997; Wang and Zhang, 2001), whereas the other considers the early Cretaceous (K_1) (e.g. Davis, 2003; Deng et al., 2003) to be more reasonable. In the following, we discuss these questions through the sequence of tectonomagmatic events in the Yanshan belt of North China.

2.2. Sequence of tectonomagmatic events and orogenic processes of the Yanshan belt, North China

The Yanshan belt of North China is an important part of the Yanshanian magmatic–metallogenic belt in East China. Based on field geology and geochronology, Davis et al. (2001) have recently established a sequence of deformational events in the Yanshan belt. Following Davis et al. (2001), we present a simplified scheme of the Yanshanian (Jura-Cretaceous) tectonomagmatic event sequence of the Yanshan orogenic belt in North China (Table 1) (modified from Deng et al., 2004a and references therein). In Table 1, we use the stage ages of

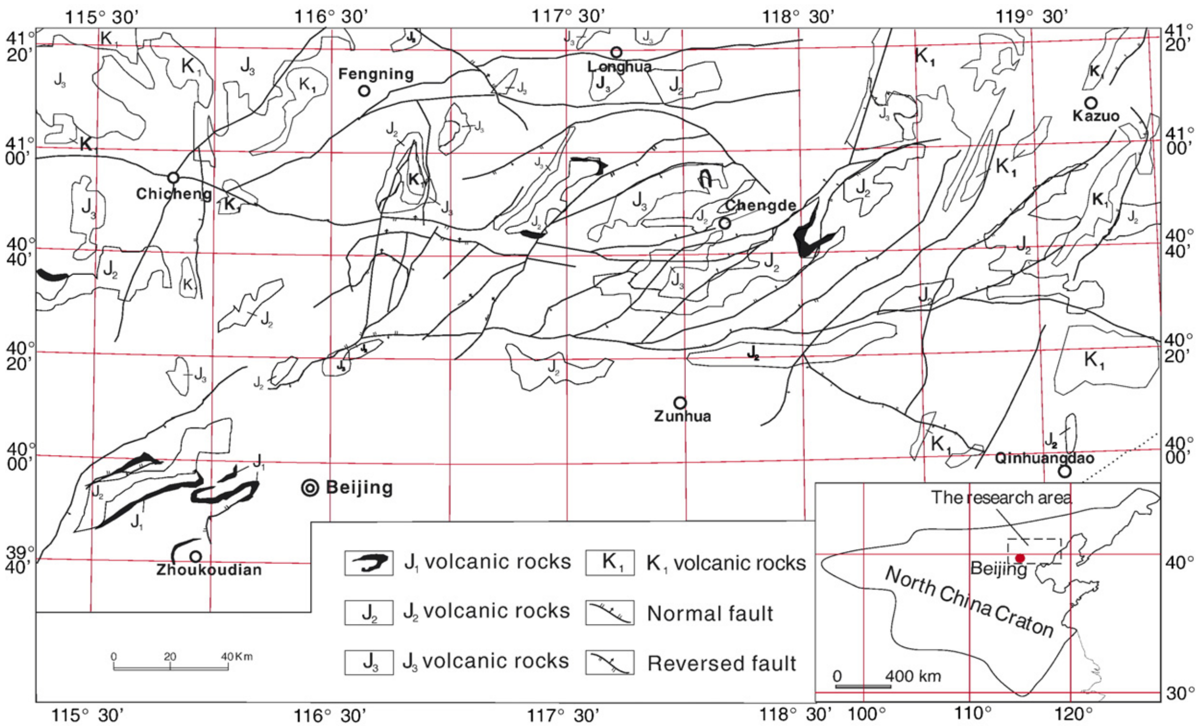

Fig. 1. Simplified map showing the distribution of volcanic rocks in the Yanshan belt. The inset shows the study area. Detailed volcanic rock names are given in Table 1.

the "International stratigraphic Chart" by Remane et al. (2000), and the geological events include the volcanic rock assemblage, sedimentary formation, intrusive rock assemblage, tectonic deformational phase, metamorphism, crustal uplift and erosion, and unconformity-forming events.

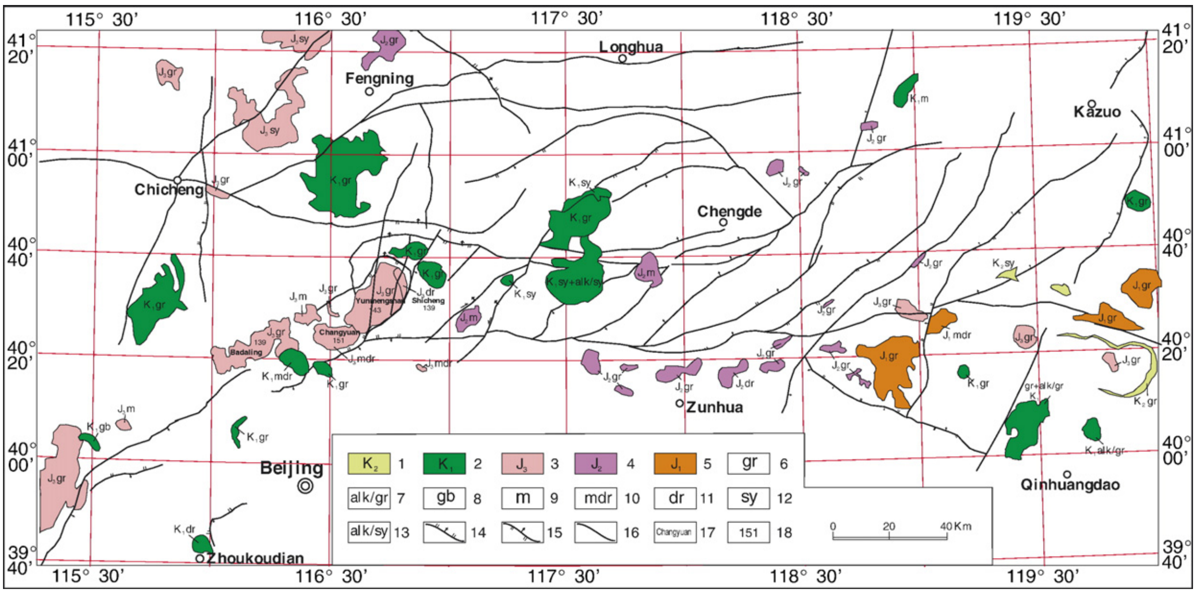

Fig. 2. Simplified map showing the distribution of intrusive rocks in the Yanshan belt. 1, K_2 intrusion; 2, K_1 intrusion; 3, J_3 intrusion; 4, J_2 intrusion; 5, J_1 intrusion; 6, granite; 7, alkaline granite; 8, gabbro; 9, monzonite; 10, monzodiorite; 11, diorite; 12, syenite; 13, alkaline syenite; 14, normal fault; 15, reversed fault; 16, geological boundary; 17, intrusion name; 18, intrusion age.

Table 1
Scheme of the Yanshanian (Jura-Cretaceous) tectonomagmatic event sequence of the Yanshan orogenic belt, North China (modified after Deng et al., 2004a and references therein)

Time		Stratigraphy	Volcanic and sedimentary formation	Intrusive rock assemblage	Tectonic deformation phase and metamorphism
	K_2	Sunjiawan	Molasse-like (?)		
96 Ma					
	K_1	Fuxin	Coal-bearing formation	al k/gr-gr (118-119 Ma), bimodal dike swarm (120-114Ma)	Late K_1^2 metamorphic core complex, Yunmengshan, 119-114 Ma, and normal faulting
		Jiufutang	Lake-basin formation		Early K_1^1 localized reverse faulting with NW-trending (<125 Ma)
		Yixian	B-TB-BTA, 135-121 Ma	gb-mgb-mdr-m-sy-alk/sy-gr (133-127Ma)	
135Ma					
	J_3	Shouwangfen	Molasse		Late J_3 NE-trending thrusting (138-136 Ma)
		Zhangjiakou	TA-T-D-R, 148-140 Ma	gb-mdr-m-qm-gr (148-136Ma)	J_3 southward thrusting (144-140 Ma) (Sihetang, Gubeikou) and amphibolite facies metamorphism (144-138 Ma)
154 Ma					
	J_2	Houcheng	Molasse	m-qm-gr (174-151Ma)	Late J_2-early J_3 northward thrust (161Ma-148Ma) (Chengde, Shisanling, Xinglong) and amphibolite facies metamorphism159-151 Ma
		Tiaojishan	TA-T-D-R, 173-161 Ma		
175 Ma					Late J_1 NEE-trend folding and thrusting (Western Hills of Beijing), andchloritoid-staurolite-kyanite metamorphism (<178-180, ≥175 Ma?)
	J_1	Jiulongshan	Molasse-like		
		Xiahuayuan	Coal-bearing formation (tuff layers, R, 180-178 Ma)		
		Nandaling	B-TB-BTA-TA-T, 196-184 Ma	m -gr (?) (199-196 Ma)	
203 Ma					
	T_3				Indosinian south-vergent thrust faulting (Pre-180 Ma or pre-199 Ma), Pingquan–Chengde–Chicheng mylonite (~211 Ma)

B, basalt; TB, trachybasalt; BTA, basaltic trachyandesite; TA, trachyandesite; D, dacite; T, trachyte; R, rhyolite; gb, gabbro; mgb, monzogabbro; mdr, monzodiorite; m, monzonite; qm, quartz monzonite; sy, syenite; alk/sy, alkaline syenite; gr, granite; alk/gr, alkaline granite; angular unconformity. The classification and nomenclatures of volcanic and intrusive rocks are after Le Maitre (1989) and Middlemost (1994), respectively. The stage ages are after Remane et al. (2000).

2.2.1. Tectonic events

The Yanshanian orogenic belt of North China is characterized by intensive contractional deformation manifested as folds, recumbent folds, reverse faults, thrust, nappes, and highly ductile shear zones (e.g. Wong, 1927; HBGMR, 1989; BBGMR, 1991; Davis et al., 2001; Yang et al., 2001; Davis, 2003; Deng et al., 2003, 2004a). For this reason, Davis et al. (2001) call the belt as a fold and thrust belt. Davis (2003) also emphasized the widespread involvement of Archean basement rocks during Yanshanian tectonism.

Three contractional deformation phases were proposed previously (e.g. HBGMR, 1989; BBGMR, 1991), but recent studies indicate four contractional deformation phases (Davis et al., 2001; Deng et al., 2003, 2004a) (see Table 1). The major contractional deformation occurred in the timeframe of 170–130 Ma (Davis, 2003) or 175–132 Ma (Deng et al., 2003, 2004a). Extensional deformation on regional scales such as normal faulting began to develop at ~118–115 Ma (Davis et al., 2001). Thus, the time period ~130–120 Ma may represent a tectonic transition.

2.2.2. Development of sedimentary basins

Table 1 shows that coal-bearing formations were developed during both J_1^1 time of the Jurassic and K_1^2 time of the Cretaceous. In the K_1^1 time of the Cretaceous, lake basins were developed. However, in the J_1^2, J_2^2 and J_3^2 times of the Jurassic, the molasse formations were developed. These three molasse formations are consistent with three phases of contractional deformation (e.g., folding and thrusting). It is unclear if the Jiulongshan (J_1^2) molasse-like formation may be related to some recognized thrusting events. The SE-limbs of the Jiulongshan and Qianjuntai syncline of the western Hills in Beijing are steeper than the NW-limbs, a geometry that may indicate NNW-plunging folding (Deng et al., 2003, 2004a). The Houcheng (J_2^2) and the Shouwangfen (J_3^2) molasses are clearly related to the thrusting and situated at the footwall of the thrust. Davis et al. (2001) call these molasses as syn-tectonic foredeep deposits. Both coal-bearing formations in J_1^1 and K_1^2 are consistent with non-contractional deformation phases, which may be consistent with the quiet tectonic environment.

2.2.3. Metamorphism

Metamorphism associated with the Yanshanian orogenesis is poorly studied, but is an important aspect of the geological history. It is well documented that the J_1 and pre-J_1 strata in the western Hills of Beijing have widely experienced chloritoid–staurolite–kyanite lower temperature–higher pressure metamorphism (BBGMR, 1991), which is considered to have occurred in late Early Jurassic (J_1^2) (<178–180 Ma, ≥175 Ma; Table 1). The J_2^2–J_3^1 Changyuan quartz monzonite of 151±2 Ma (single zircon U–Pb age by Davis et al., 2001) and 152.7±3.2 Ma (SHRIMP zircon U–Pb age by Deng et al., 2004a) and Shicheng monzonite of 159±2 Ma (single zircon U–Pb age by Davis et al., 2001) and 155.8±1.5 Ma (SHRIMP zircon U–Pb age by Deng et al., 2004a) are in fact gneisses of amphibolite facies, where magmatic textures were almost totally eliminated. The Shantuozi granite of 151±2 Ma (single zircon U–Pb age by Davis et al., 2001) is a syn-tectonic pluton and has been metamorphosed to augen gneiss. Some of the J_3 Yunmengshan granitic intrusions of 143±4 Ma (single zircon U–Pb age by Davis et al., 2001) and 144.7±2.7 Ma (SHRIMP zircon U–Pb age by Deng et al., 2004a) and the Wudaohe granitic platoon of 141±2 Ma (single zircon U–Pb age by Davis et al., 2001) are also metamorphic augen gneisses.

It is obvious that the three episodes of the metamorphism are spatially and temporally associated with the three contractional deformation phases (see Table 1). The monzonitic, quartz monzonitic and granitic gneisses are exposed deep crustal rocks, suggesting the J_2^2 and J_3^2 contractional deformation affected deep crustal levels (Davis et al., 2001).

2.2.4. Igneous rock assemblage

The igneous rock assemblages, shown in Table 1, will be discussed in a later section.

2.3. Orogenic episodes and crustal tectonic thickening

2.3.1. Five orogenic episodes

Five orogenic episodes have been recognized on the basis of tectonic activities (including unconformities), basin formations, metamorphism and igneous rock assemblages (Table 1) (modified from Deng et al., 2003, 2004a).

2.3.1.1. J1: pre- and initial orogenic episode. Deng et al. (2004b) suggest pre-orogenic extension as manifested by basalts, trachy-basalts and basaltic trachyandesites erupted along two triple junction-like rift systems (Fig. 3). This is followed by sedimentary basin development as indicated by the coal-bearing sedimentary strata, probably reflecting a quiet tectonic environment. The subsequent molasse-like formations and metamorphism resulted from the contractional deformation. Finally, the uplifting and erosion resulted in the unconformity with the overlaying J_2 strata.

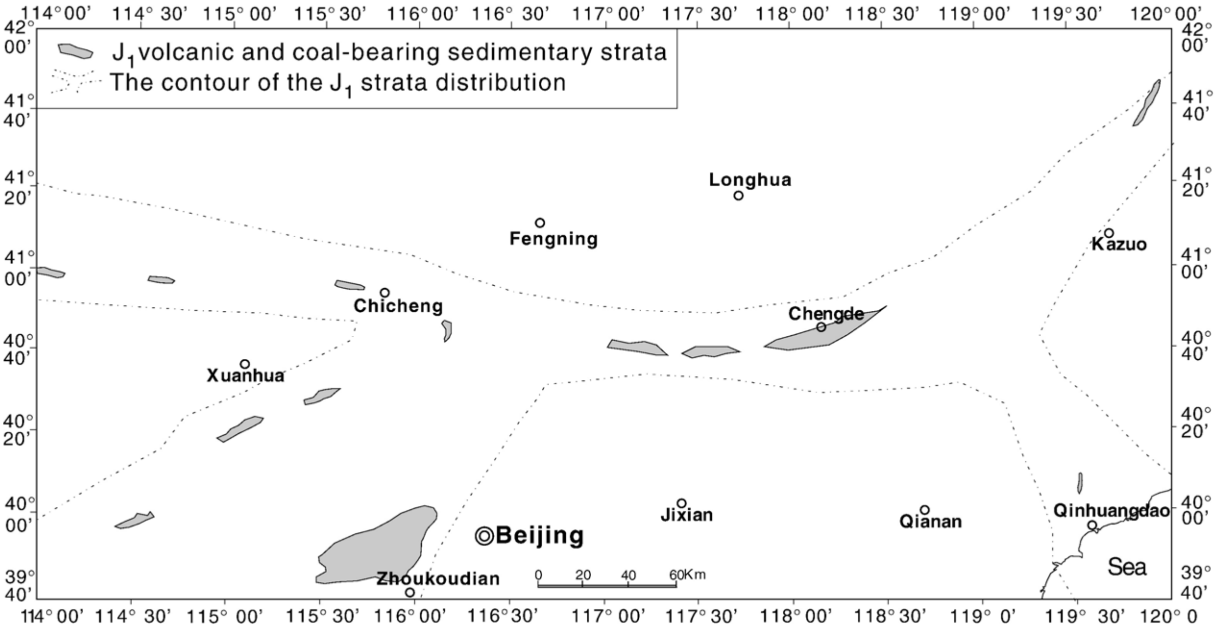

Fig. 3. The distribution of early Jurassic (J_1) volcanic rocks and coal-bearing sedimentary formations in the Yanshan orogenic belt.

2.3.1.2. J2: early orogenic episode. This episode began with rifting-associated volcanism (Davis et al., 2001) followed by molasse sedimentation, syn-tectonic plutonism and deep crustal level metamorphism as a result of contractional deformation. The episode ended with uplifting and erosion as recorded by the unconformity with the overlaying J_3 strata. In contrast to the J_1 orogenic episode, the J_2 episode is also accompanied by the emplacement of high-pressure trachyte (and latite) and syenite (and monzonite) formed at the base of the thickened crust (see next section).

2.3.1.3. J3: peak orogenic episode. This episode began with large-scale regional volcanism followed by molasse formation, syn-tectonic plutonism, metamorphism, and contractional deformation. The final stage of the episode is again characterized by uplifting, erosion and the development of the future unconformity with the overlaying K_1^1 strata.

2.3.1.4. K1^1: late orogenic episode. The Late orogenic episode resembles the J_3 episode, but differs in important ways: (a) thrusting is limited in scale and the metamorphism is less intense, (b) wide-spread development of lake-basin sedimentation in a tectonically quiet environment instead of the molasse formation, and (c) emplacement of alkaline amphibole-bearing syenite and alkaline feldspar granite with miarolitic texture in some localities.

2.3.1.5. K12: post-orogenic episode. In this episode, volcanic eruption is scattered, and the regional deformation is characterized by extensional (vs. contractional) features along with the development of coal-bearing sedimentation, typical metamorphic core complex (e.g. Davis et al., 2001) and post-orogenic alkaline granite and bimodal dike swarms. We suggest that these geological phenomena reflect orogenic collapses.

2.3.2. Crustal thickening by tectonism

The foregoing discussion indicates significant crustal shortening and thickening as a result of contractional deformation during the initial stages of J_1^2, J_2^2 and J_3^2 tectonic episodes. All these were followed by a tectonic regime change (i.e., the late orogenic episode (K_1^1) towards the development of large-scale deformation during the post-orogenic episode (K_1^2) of the Yanshanian orogenesis.

The thickness of the tectonically thickened crust is difficult to estimate on the basis of contractional deformation alone, but can be inferred from the petrology and geochemistry of genetically associated igneous (and metamorphic) rocks and rock assemblages (see next section).

2.3.3. The P–T–t path of the orogenic processes: mantle-derived heat for crustal melting

Brown (1993, 1994) suggests two fundamentally different types of orogenic belt defined by relative

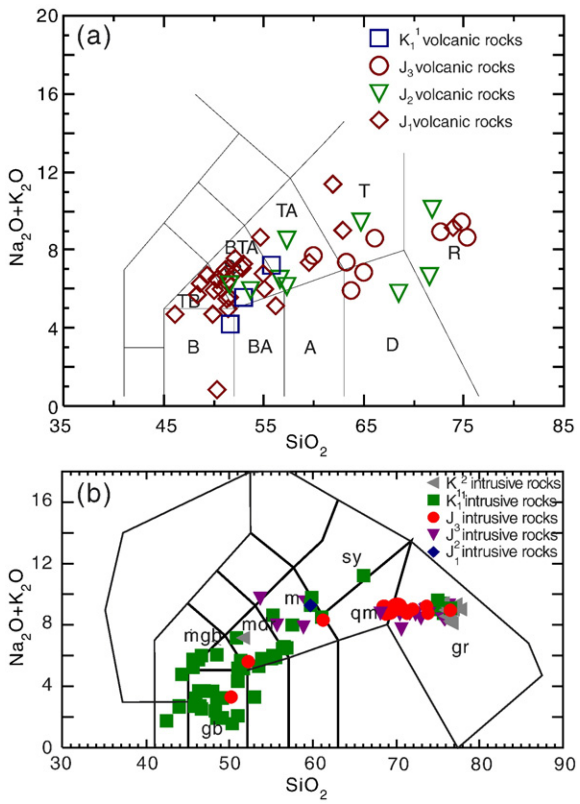

Fig. 4. Chemical classification and nomenclatures of volcanic (a) and intrusive (b) rocks using the total alkali versus silica (TAS) diagram (e.g., Le Maitre, 1989; Middlemost, 1994) of the Yanshan belt. Data are from Wang and Jin (1990), Bai et al. (1991), Wang et al. (1994) and J.-F. Deng's unpublished data.

timing of maximum ***T*** and maximum ***P***. In the orogenic belt characterized by *CW* (clockwise) P–T path metamorphism, granite is formed during the middle and late stages. For orogenic belt characterized *CCW* (counterclockwise) metamorphism, however, granite is generated pre- or early syn-tectonic stage. Thus, the evolution of orogenic belts may be interpreted from the metamorphic rocks. Alternatively, Deng et al. (2002) suggest that the P–T–t path of the orogenic processes may be derived directly from the tectonomagmatic event sequence. The *CW* orogenic belt is characterized by early contractional deformation before magmatic activity, whereas the *CCW* orogenic belt is characterized by early magmatism before contractional deformation.

Each orogenic episode, except for the latest post-orogenic episode, corresponds to a short cycle of the tectonomagmatic event. It began with volcanic eruption and plutonism, through sedimentation, to deformation and metamorphism, and ended with uplifting and erosion. Each of this cycles is followed a counterclockwise (*CCW*) P–T–t path with time, i.e. heating the crust from mantle, followed by crustal thickening from the contractional deformation, and finally by uplifting and erosion resulting in decompression of the crust. Therefore crust heating predates the contractional deformation. Mantle-derived heat must have weakened and changed the rheology of the existing cratonic crust, thus facilitating contractional deformation and crustal thickening. Metamorphic rocks that experienced a prograde metamorphism shows both temperature and pressure increase with time (Table 1) from J_1 to J_3, which suggests the crust being progressively heated and thickened, and finally resulting in the peak orogenic episode during late Jurassic (J_3).

3. Igneous petrotectonic assemblage of the Yanshan belt, North China

3.1. Igneous petrotectonic assemblage

The classification and nomenclature of volcanic and intrusive rocks from the Yanshan belt are given in Table 1. Fig. 4 shows that the volcanic assemblage overall consists of basalt (B)–trachybasalt (TB)–basaltic trachyandesite (BTA)–trachyandesite (TA)–trachyte (T)–dacite (D)–rhyolite (R) (Fig. 4a). The intrusive rocks include gabbro (gb), monzogabbro (mgb), monzodiorite (mdr), monzonite (m), quartz monzonite(qm), syenite (sy), alkaline syenite (alk/sy), granite (gr), and alkali granite(alk/gr) (Fig. 4b). These rocks in SiO_2–K_2O space (Fig. 5) show mainly high-K to Calc-alkaline characteristics, but can be ascribed to Calc-Alkaline (CA) and tholeiitic (TH) series in SiO_2–FeO/MgO space (Fig. 6). The overall compositional trend is steeper than

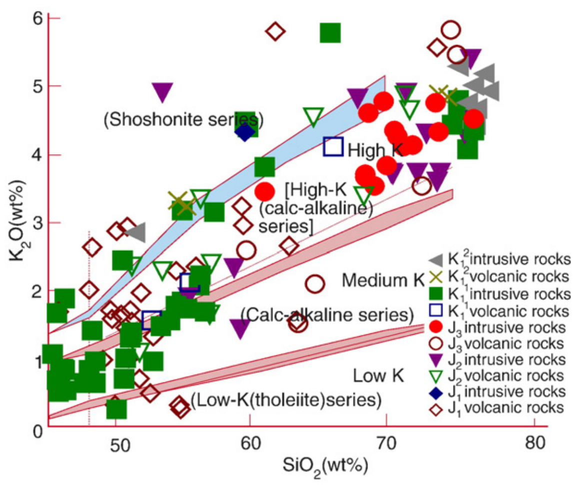

Fig. 5. SiO_2 vs. K_2O diagram (after Rollinsion, 1993) for igneous rocks of the Yanshan belt. Data are as in Fig. 4.

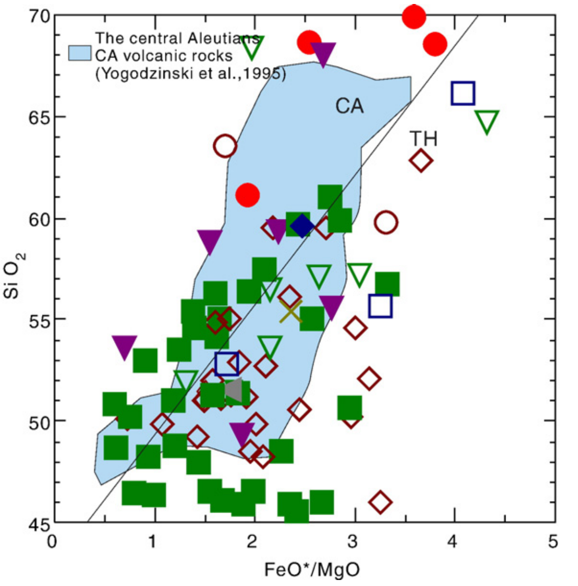

Fig. 6. SiO_2 vs. FeO/MgO diagram (after Miyashiro, 1974) for igneous rocks of the Yanshan belt. Data are as in Fig. 4. Symbol are as in Fig. 5.

that of the CA and TH (Fig. 6) boundary line defined by Miyashiro (1974), and is similar to the trend defined by the central Aleutian arc CA (Yogodzinski et al., 1995). On modified (after Frost et al., 2001) Peacock diagram, the Yanshan belt igneous rocks are mainly alkali-calcic rock series (Fig. 7).

As shown in Table 1, (1) the pre- and initial orogenic episode (J_1) is characterized by the assemblage of B–TB–BTA–TA–T–R volcanic and m–gr intrusive rocks, (2) the early orogenic episode (J_2) by the assemblages of TA–T–D–R volcanic and m–qm–gr intrusive rocks, (3) the peak orogenic episode (J_3) by the assemblages of TA–T–D–R volcanic and gb–mdr–m–qm–gr intrusive rocks, (4) the late orogenic episode (K_1^1) by the assemblages of B–TB–BTA volcanic and gb–mgb–mdr–m–sy–alk/sy–gr intrusive rocks, and (5) the post-orogenic episode by the bimodal dike swarms and alk/gr–gr assemblage.

The significance of such petrotectonic assemblages is several-fold: (1) during the pre- and initial orogenic episode (J_1), B–TB–BTA assemblage dominates with lesser amounts of felsic rocks. This, together with the low-T and high-P chloritoid-grade metamorphism, suggests the volumetrical significance of mantle-derived basaltic melts that underplate and heat the cold and strong Archean cratonic crust; (2) however, during the early and peak orogenic episodes (J_2 and J_3), magmatism is wide-spread and is dominated by TA–T–R and m–qm–gr. This igneous assemblage, together with relatively high-T amphibolite facies metamorphism, indicates that the crust is already heated to higher temperatures. The dominance of TA and m with lesser B–TB–BTA and gb–mgb–mdr may be a tectonic response to the strongly contractional deformation during J_2 and J_3. We reason that such contractional regime may favor deep crustal level trapping of underplating basaltic magmas, crustal assimilation and felsic magma generation, including that of trachyandesitic composition; (3) the late orogenic episode (K_1^1) is magmaticaly dominated by B–TB–BTA and gb–mgb–mdr assemblages with alk/sy, which is consistent with the tectonic regime transitional from contractional to extensional phases; (4) the development of bimodal dike swarms and alk/gr–gr in K_1^2 is interpreted to characterize post-orogenic regional extensional settings.

3.2. High-pressure trachyte and syenite, and thickened continental crust

On the basis of phase equilibria, Wyllie (1977, 1984) indicated that trachyte (and syenite) (vs. granite) magmas are formed from partial melting of crustal rocks at the base of thickened continental crust at depths in excess of 50 km. Using the available experimental data, Deng et al. (1998, and references therein) presented a diagram showing water-undersaturated liquidus surface for trachyte (and syenite) melts (Fig. 8). Fig. 8 suggests that at >15 kb pressure the high-pressure trachytic and syenitic melts may be generated by (1) partial melting of crustal partial with eclogitic residues or (2) fractional crystallization of underplating basalts with eclogitic cumulates. Thus, it is conceivable that the hypothesized eclogites as melting residues or cumulates may be formed beneath the thickened crust. Fig. 8 shows that high-pressure trachyte and syenite melts formed at >15 kb pressures would show no

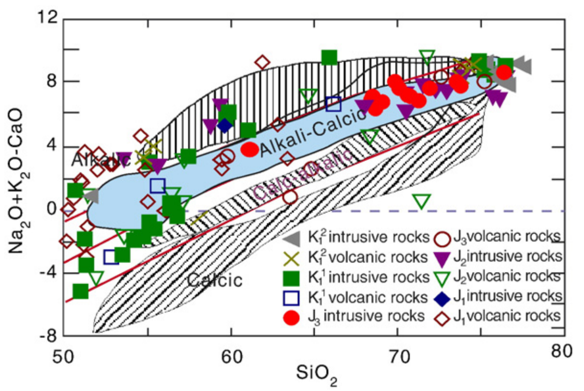

Fig. 7. Modified alkali-lime Peacock index diagram (after Frost et al., 2001) for igneous rocks of the Yanshan belt. Data are as in Fig. 4.

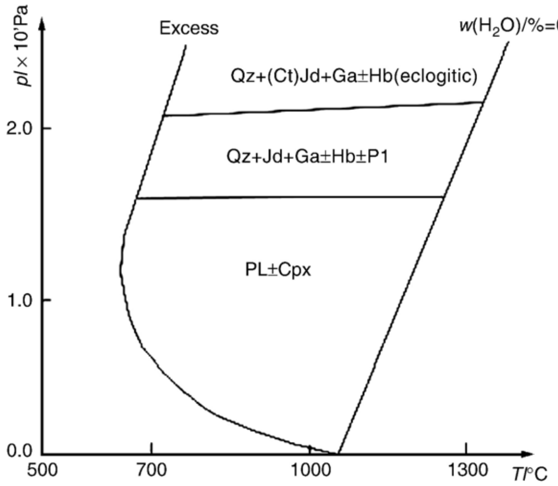

Fig. 8. Schematic illustration of water-undersaturated liquidus surface for trachyte and syenite showing liquidus and near-liquidus minerals (after Deng et al., 1998, and references therein). Pl, plagioclase; Qz, quartz, ct, coesite; cpx, clinopyroxene; Jd, jadeite and jadeitic pyroxene; Hb, hornblende; Ga, garnet.

negative Eu-anomaly because of eclogitic residues without plagioclase, which requires thickened continental crust. It is noteworthy, however, that the proposed slab melting and adakitic melts at ≥15 kb pressures may also show no negative Eu-anomaly and high Sr/Y (e.g. Drummond et al., 1996). The alkali-rich nature of the rocks we study would resemble in someway "adakitic rocks" formed at the base of thickened continental crust rather than "adakites" genetically associated with slab melting (Castillo, 2006).

Table 2 suggests that (1) except for J_1, the Yanshan belt igneous rocks from J_2 to K_1^1 have high-pressure trachytic and syenitic components, such as J_2 (WM03-10, TA), J_2/J_3 (Wy-26, qm), J_3 (wy-60, qm), J_3 (xs-11, T), K_1^1 (Wy-4, sy); (2) these high-pressure trachytic and syenitic rocks of the Yanshan belt differ from the Cenozoic adakites in $Na_2O+K_2O–SiO_2$, $SiO_2–MgO$, $SiO_2–FeO/MgO$, $SiO_2–K_2O$ diagrams, Ni content, and K_2O/Na_2O ratios; (3) the higher MgO, Ni, and the lower FeO/MgO, K_2O, K_2O/Na_2O for the adakites may result from interaction between slab melt and mantle wedge peridotites; (4) in contrast with the adakites, the lower MgO, Ni, and the higher FeO/MgO, K_2O, K_2O/Na_2O for the high-pressure trachytic and syenitic rocks are consistent with their being parental melts or derivatives of such melts likely formed at the base of thickened continental crust. Such melts would have not interacted with mantle peridotites.

Recently, Fan et al. (1998) presented the first zircon U–Pb dating of 140–120 Ma for the mafic lower crust xenoliths in the Cenozoic Hannuoba basalt. Wilde et al. (2003) presented more zircon U–Pb age dates with the peak between 180 Ma and 80 Ma for mafic and felsic granulites, and pyroxenite xenoliths. Chen et al. (2001) calculated P–T conditions (72-pairs of 9-samples of Cr-spinel garnet pyroxenite±olivine), ranging from ~15 kb and ~993 °C to ~25 kb and 1265 °C, mainly at 16–22 kb, corresponding to a depth interval of 50–65 km.

The above discussion suggests that the thickened continental crust of about 50–65 km thick may have resulted from contractional deformation during syn-orogenic episodes ($J_2–K_1^1$).

4. The thermal consideration

We know that for large-scale continental felsic and silicic magma generation, introduction of mantle-derived mafic magmas into the crust is required to provide the needed heat. Bergantz (1989) did a quantitative analysis using a one-dimensional conductive heat transfer model at 1 GPa. In this model, he took 1250 °C as the temperature of the underplating basaltic melt, and 700 °C as the mean temperature of the lower crustal country rock. He indicates that the efficiency of the underplating can be estimated in terms of the ratio of the total amount of melt generated in the country rock to the total amount of basaltic melt crystallized. This ratio may reach 0.4 for tonalite to 0.6 for metapelite. That is, to generate ~500 km^3 of peraluminous (S-type) granitic magma from a metapelite source rock requires at least 833 km^3 of basaltic melt underplated and completely crystallized, and if only 25% of the melted region was above the contiguity limit, over 3333 km^3 of underplated basalt would be required to yield 500 km^3 of extractable magma. Bergantz concluded that simple underplating of metapelite by basalt melts can yield magma bodies with melt fractions in excess of the rheological limit of extraction for almost any reasonable geotherm. However, granitic and tonalitic protoliths do not appear to yield substantial amounts of extractable magma. He thus suggests that underplating may represent repeated intrusion or occurs in deep crustal levels in order to yield magma bodies from granitic and tonalitic protoliths. Tepper et al. (1993) used the Bergantz's one-dimensional model for generating calc-alkaline granitoids of the Chilliwack batholith in North Cascades by melting mafic lower crust, the results of which indicate that underplating of basaltic magmas can provide the heat required for large-scale melting of amphibolitic lower crust, provided that the ambient wall-rock temperatures exceed 800 °C. This model may be applicable to other Cordilleran batholiths.

Table 2
Representative mean compositions of igneous rocks with 70 wt.%>SiO_2≥57 wt.% of the Yanshan belt and the average Cenozoic adakite

	The Yanshan belt												The average Cenozoic adakite (n=140)
	Volcanic rocks						Intrusive rocks						
No.	WM03–14	WM03–10	WM03–21	WM03–3	WM03–17	XS-11	WY-62	YS-23	WY-26	WY-60	WM03-26	WY-4	
Age	J_1 184.1 ±4.5 Ma	J_2 160.7 Ma	J_2 166.7 ±3.2 Ma	J_3* 144.7 ±4.8 Ma	J_3 137.3 Ma	J_3* 138 Ma	J_1 196.5 ±1.9 Ma	J_2 159.3 ±1.9 Ma	J_2/J_3 152.7 ±3.2 Ma	J_3 137.6 ±1.2 Ma	J_3 136 Ma	K_1^1 124.2 ±1.8 Ma	
SiO_2(wt.%)	62.85 (T)	57.23 (TA)	64.67 (T)	66.16 (T)	59.8 (TA)	63.42 (T)	59.62 (m)	67.98 (qm)	61.12 (qm)	68.69 (qm)	69.86 (qm)	59.85 (sy)	63.84 (D)
MgO(wt.%)	1.35	2.24	0.91	0.95	1.78	0.99	2.39	1.37	2.88	1.13	0.80	1.45	2.47
FeO/MgO	3.66 (Th)	3.04 (Th)	4.32 (Th)	4.07 (Th)	3.31 (Th)	5.21 (Th)	2.48 (CA)	2.69 (CA)	1.91 (CA)	2.54 (CA)	3.59 (CA)	2.85 (CA)	1.70 (CA)
SiO_2–K_2O relation	HK CA	HK CA	SH	SH	HK CA	MK CA	SH	HK CA	HK CA	HK CA	HK CA	SH	MK CA
K_2O/Na_2O	0.42	0.39	0.94	0.91	0.51	0.28	0.89	1.24	0.71	1.13	1.07	0.82	0.35
Sr (ppm)	336	838	606	238	794	1004	690	370	899	842	467	1348	869
Y (ppm)	15.9	16.5	17.1	18.9	23.8	21.7	40.5	19.4	16.7	8.01	18.9	15.4	9.5
Sr/Y	21.13	50.79	35.44	12.59	33.36	46.27	17.04	19.07	53.83	105.12	24.71	87.53	91.47
δEu	0.89	0.84	0.76	0.78	0.83	1.0	0.77	0.56	0.88	1.09	0.57	1.99	
Ni(ppm)	2.63	15.1	1.56	6.01	2.09	2.59	15.7	11.8	25.61	4.77	4.20	2.72	39.0
Source	this paper, unpublished data												Drummond et al., 1996

The ages are SHRIMP zircon U–Pb age of the sample. Those with * are not the sample age, but the age of the same strata nearby. The classification and nomenclatures of volcanic and intrusive rocks are after Le Maitre (1989) and Middlemost (1994), respectively. T, trachyte; TA, trachyandesite; D, dacite; m, monzonite; qm, quartz monzonite; sy, syenite; Th, CA are tholeiitic and calc-alkali series after SiO_2–FeO/MgO relation from Miyashiro (1974). The FeO/MgO, K_2O/Na_2O and Sr/Y are calculated in this paper from the average composition of the Cenozoic adakite of Drummond et al. (1996).

Our preliminary modeling following Bergantz (1989) shows that the ratio of the granitic melt generated in the tonalitic lower crust over the total amount of the underplated basaltic magma crystallized is about 0.12 for a basaltic magma of 1250 °C at 1 GPa and by assuming 400 °C of the tonalitic lower crust (Liu, 2004). The 400 °C of the tonalitic lower crust at 1 GPa is suggested based on the cratonic geotherm of the North China before the Yanshan orogenesis (Wyllie, 1977; Griffin et al., 1998). The ratio of 0.12 is much less than the Bergantz's ratio of 0.4 for the tonalitic protolith because of much cooler lower crust (~400 °C) than in Bergantz's model for the tonalitic protolith. Therefore, the large amount of basalts intruded by the repeated basaltic magma underplating for large-scale granitic magma generation in the Yanshan belt is required.

We envision that the large-scale granitic magma generation beneath the North China Craton began after the cratonic lower crust had been heated up to ~800 °C by the underplating/underplated basaltic magmas. Based on elemental budget and mass balance calculations, Gao et al. (1998) suggest that a cumulative 37–82 km thick eclogitic lower crust must have been emplaced and then removed by delamination in order to explain the relative Eu, Sr and transition metal deficits in the crust of central East China, and the paucity of eclogite and mantle peridotite xenoliths associated with the Cenozoic volcanism in East China. The early Jurassic evolved basaltic and trachybasaltic volcanic eruptions (Table 1) suggest that the repeatedly underplating mantle melts were not fully crystallized. This, plus the limited rhyolite and granite occurrences in J_1 and the lower temperature chloritoid-grade metamorphism in late J_1 (Table 1), suggests the predominance of cratonic lower crust heating during this time (J_1). The large-scale felsic and silicic magma eruptions and intrusions, as well as the higher amphibolite metamorphism, became important in the J_2 time (Table 1), suggesting that the cratonic crust became adequately hot since latest J_1 or early J_2.

In summary, we emphasize that (1) underplating of volumetrically significant basalt magma is required; (2) the underplating initially (J_1) heated up the otherwise relatively cold Archean crust to temperatures up to ~800 °C; (3) the underplating continued throughout the Jurassic to early Cretaceous, which explains the genesis of large-scale felsic magmatism during J_2, J_3, K_1^1 (Table 1); (4) Some or much of the underplated basaltic melts and their cumulates may have transformed to dense eclogites at deep levels of the thickened crust in response to the contemporary contractional deformation events. (5) The latter and the eclogitic residues and/or cumulates generated in the formation of the high-pressure trachytic and syenitic melts would facilitate the future delamination although details of these processes remain to be investigated.

5. A possible model for the lithospheric thinning of North China Craton: delamination

5.1. The regional tectonic framework

The regional tectonic development may have provided the needed conditions for the reactivation of the North China Craton during the Jura-Cretaceous (i.e. Yanshanian) time. According to Van der Voo et al. (1999), the Mongolia–North China–South China blocks amalgamated during the Permian-Triassic periods. This amalgamated tectonic block was then surrounded by oceanic subduction zones and was accreted to the Siberia Craton during Jura-Cretaceous time. Thus, during the Yanshanian stage, the North China Craton is generally situated in a subduction–collisional-related tectonic regime, which is consistent with magmatism and tectonism of orogenic style. Therefore, this regional tectonic regime may have provided a basic framework for the lithospheric thinning of North China (see below).

5.2. The delamination model

The fact that the continental crust is on average much older than the oceanic crust is simply because the former has been protected by the similarly old subcontinental lithosphere from the convective asthenosphere. This is the case because the subcontinental lithosphere is compositionally depleted/refractory and physically buoyant (i.e., low FeO/MgO and low Al_2O_3 etc.). Therefore, for such subcontinental lithospheric mantle to delaminate is physically not straightforward (Niu et al., 2003; Niu, 2005). However, the observation that the subcontinental lithosphere has indeed been thinned in the Mesozoic in eastern China requires a physically sound explanation. Niu (2005) emphasizes the importance of hydration of the basal lithosphere, which changed the rheology of the basal lithosphere and thus transformed the lithosphere into asthenosphere. Here we emphasize the importance of the process that may have increased the density of the lithosphere, thus allowing its portion to founder into the asthenosphere, i.e., the thinning of the lithosphere.

Kay and Kay (1993) suggested that for regions with thin crust (<50 km), the lower crust of any composition remains less dense than the underlying mantle. In

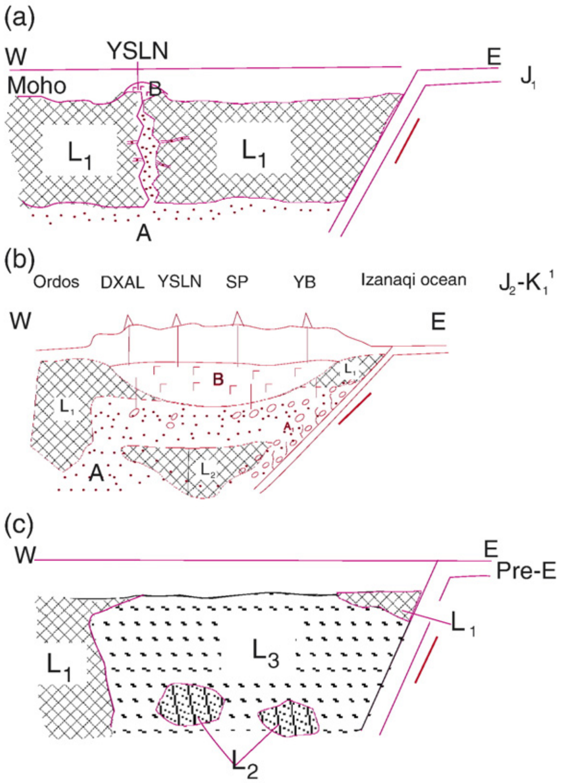

Fig. 9. The delamination model showing the evolution of the lithosphere beneath North China during Jura-Cretaceous time (modified from Deng et al., 2003). (a) basaltic magma (B) ascending from asthenosphere (A) along the ruptures of the cratonic lithosphere (L_1) and underplating at the base of the crust, resulting in the volcanism in the Yanshan-Western Liaoning area (YSLN). (b) regional lithospheric delamination (L_2) and upwelling of the asthenosphere (A), resulting in the widespread volcanism, including Daxinganling (DXAL), YSLN, Siping (SP), and Yanbian (YB) to the east and northeast of the Ordos block. (c) the composite lithosphere ($L_1+L_2+L_3$) is formed, the L_3 is the new lithosphere formed as a result of more recent (pre-Eogene?) asthenospheric cooling.

contrast, in regions where the crust may have been thickened to >50 km through tectonic compression, rocks of basaltic composition in the lower crust would be metamorphosed to dense eclogites. We argue above that underplating of volumetrically significant amount of basaltic magma is required to explain the large-scale crustal melting in the Mesozoic eastern China. We further argue that the multiple episodes of contractional deformation must have resulted in the crustal thickening, perhaps in excess of 50–65 Km during J_1^2–K_1^1 time. This allows the basal underplated basalts and their cumulates to metamorphose into the dense eclogites, facilitating possible delamination. We note however that such eclogite driven delamination requires significant prior lithospheric mantle removal. This is because the hypothesized eclogite layer may not sink through the compositionally depleted/refractory and physically buoyant lithospheric mantle that may be in excess of >150 km thick. The possible delamination model is shown in Fig. 9.

We suggest a delamination model showing the evolution of the lithosphere beneath North China during Jura-Cretaceous time (Fig. 9). During J_1, basaltic magmas ascended from the asthenosphere along ruptures or zones of weakness of the cratonic lithosphere (L_1) and underplated at the base of the crust, resulting in the volcanism in the Yanshan-western Liaoning area (YSLN) (Fig. 9a). During J_2–K_1^1, regional scale lithospheric delamination (L_2) took place, and as a result asthenosphere (A) upwelling led to widespread volcanism, including Daxinganling (SXAL), YSLN, Siping(SP), and Yanbian(YB) to the east and northeast of the ordos block (Fig. 9b). The composite lithosphere ($L_1+L_2+L_3$) is finally formed, the L_3 is the new lithosphere formed as a result of more recent (Pre-Eogene?) asthenospheric cooling (Fig. 9c).

We may come to the following conclusions: (1) underplating basaltic magmas heat and weaken the existing cold and strong crust, which would facilitate contractional deformation and crustal thickening; (2) the contractional deformation is necessary to thicken the crust, and to transform the underplated basaltic rocks into eclogites; (3) the input of the large amount of the basaltic magmas into the craton is required to cause crustal melting; (4) the combination of above (2) and (3) is necessary for the formation of large amount of eclogites, and then to transform the buoyant continental root into dense one for the subsequent delamination, (5) the combined subduction–collision-related tectonic setting may be ideal for cratonic lithospheric thinning.

Acknowledgments

This work is supported by NSF of China (No. 40234048), the project of Chinese Geological Survey (No. 200113900018), the project of the Ministry of Land and Mineral Resources (No.20001010202), and the project of the Ministry of Science and Technology (No. 2001cb711002). We acknowledge that the discussion with, and comments by, the IUGS-SECE conference participants helped significantly for improved understanding of the crustal–mantle interaction processes presented in this paper. We would also like to thank the constructive comments by Zhengfu Guo and Shan Gao, which have improved both scientific presentation and readability of the paper.

References

Bai, Z.M., Xu, S.Z., Ge, S.W., 1991. Badaling granitic complex. Geol. Pub. House, pp. 1–172 (in Chinese).

BBGMR (Beijing Bureau of Geology and Mineral Resources), 1991. Regional geology of Beijing Municipality. Geol. Pub. House, Beijing, pp. 1–598 (in Chinese with English abstract).

Bergantz, G.W., 1989. Underplating and partial melting: implications for melt generation and extraction. Science 245, 1093–1095.

Brown, M., 1993. P–T–t evolution of orogenic belts and the causes of regional metamorphism. J. Geol. Soc. (Lond.) 150, 227–241.

Brown, M., 1994. The generation, segregation, ascent and emplacement of granite magma: the migmatite-to-crustally-derived granite connection in thickened orogenes. Earth Sci. Rev. 36, 83–130.

Castillo, P.R., 2006. An overview of adakite petrogenesis. Chin. Sci. Bull. 51, 257–268.

Chen, S.H., O'Reilly, S.Y., Zhou, X.H., et al., 2001. Thermal and petrological structure of the lithosphere beneath Hannuoba, Sino-Koreau Craton, China: evidence from xenoliths. Lithos 56, 267–301.

Chen, B., Zhai, M.G., Shao, J.A., 2002. Petrogenesis and significance of the Mesozoic North Taihang complex: major and trace element evidence. Sci. China, Ser. D: Earth Sci. 32, 896–907 (in China).

Chen, B., Jahn, B.M., Zhai, M.G., 2003. Sr–Nd isotopic characteristics of the Mesozoic magmatism in the Taihang-Yanshan orogen, North China Craton, and implications for Archean lithosphere thinning. J. Geol. Soc. (Lond.) 160, 963–970.

Chen, B., Tian, W., Zhai, M.G., Arakawa, Y., 2005. Zircon U–Pb geochronology of the Mesozoic magmatism in the Taihang mountain and other places of the North China Craton, with implications for petrogenesis and geodynamic setting. Acta Petrol. Sin. 21 (1), 13–24 (in Chinese with abstract).

Davis, G.A., 2003. The Yanshan belt of North China: tectonics, adakitic magmatism, and crustal evolution. Earth Sci. Front. (CUGS) 10 (4), 373–384.

Davis, G.S, Zhang, Y.D., Wang, C., et al., 2001. Mesozoic tectonic evolution of the Yanshan fold and thrust belt, with emphasis on Hebei and Liaoning Provinces northern China. GSA Memoir 194, 171–197.

Deng, J.F., 1988. Continental rift magmatism and deep process. In: Chi, J.-S. (Ed.), Cenozoic basalt and upper mantle of eastern China. China University of Geosciences Press, Wuhan, pp. 201–218 (in Chinese).

Deng, J.F, Mo, X.X., Zhao, H.L., Luo, Z.H., Du, Y.S, 1994. Lithosphere root/de-rooting and activation of the East China continent. Geoscience 8 (3), 349–356 (in Chinese, with English abstract).

Deng, J.F, Zhao, H.L., Mo, X.X., et al., 1996. Continental Roots-Plume Tectonics of China: Key to Continental Dynamics. Geol. Pub. House, Beijing, pp. 1–110 (in Chinese, with English abstract).

Deng, J.F, Luo, Z.H, Zhao, H.L., 1998. Trachyte and syenite: petrogenesis constrained by the petrological phase equilibrium. Depart. Geol. Peking Univ., Collected works of international symposium on geological science held at Peking University. Seismolog. Pub. House, Beijing China, pp. 745–757.

Deng, J.F, Mo, X.X, Xiao, Q.H., et al., 2002. Sequence of geological events and PTt paths of orogenic processes. Acta Petrol. Miner. 21 (4), 336–342 (in Chinese, with English abstract).

Deng, J.F, Su, S.G., Mo, X.X., 2003. Deep processes of Mesozoic Yanshanian lithosphere thinning in North China. Earth Sci. Front. (CUGS) 10 (3), 41–50.

Deng, J.F, Su, S.G., Mo, X.X., et al., 2004a. The sequence of magmatic-tectonic events and orogenic processes of Yanshan belt, North China. Acta Geol. Sin. 78 (1), 260–266.

Deng, J.F, Su, S.G., Zhao, G.C., et al., 2004b. Structured elements association of Yanshan orogenic belt, North China. Geol. J. China Univ. 10 (3), 315–323 (in Chinese with English abstract).

Deng, J.F, Mo, X.X, Zhao, H.L., et al., 2004c. A new model for the dynamic evolution of Chinese lithosphere: "Continental roots-plume tectonics". Earth Sci. Rev. 65, 223–275.

Drummond, M.S., Defant, M.J., Kepezhinskas, P.K., 1996. Petrogenesis of slab-derived trondhjemite–tonalite–dacite/adakite magma. Trans. Roy. Soc. Edinburgh: Earth Sci. 87, 205–215.

Fan, Q.-C., Liu, R.-X., Li, H.-M., Li, N., Sui, J.-L., Lin, Z.-R., 1998. Zircon chronology and REE geochemistry of granulite xenolith at Hannuoba. Chin. Sci. Bull. 43, 1510–1515.

Frost, B.R., Barnes, C.G., Collins, W.J., Arculus, R.J., Ellis, D.J., Frost, C.D., 2001. A geochemical classification for granitic rocks. J. Petrol. 42 (11), 2033–2048.

Gao, S., Zhang, T.-C., Luo, Z.-J., et al., 1992. Chemical composition of the continental crust in the Qinling orogenic belt and its adjacent North China and Yangtze cratons. Geochim. Cosmochim. Acta 56, 3933–3950.

Gao, S., Zhang, B.-R., Jiu, Z.-M., Kern, H., Luo, T.-C., Zhao, Z.-D., 1998. How mafic is the lower continental crust? Earth Planet. Sci. Lett. 161, 101–117.

Gao, S., Rudnick, R.L., Yuan, H.-L., et al., 2004. Recycling lower continental crust in the North China Craton. Nature 432, 892–897.

Ge, X.-Y., Li, X.-H., Chen, Z.-G., Li, W.-P., 2002. Geochemistry and petrogenesis of Jurassic high Sr/lower Y granitoids in eastern China: constraints on crustal thickness. Chin. Sci. Bull. 47, 474–480 (in Chinese).

Griffin, W.L., Zhang, A., O'Reilly, S.Y., Ryan, C.G., 1998. Phanerozoic evolution of the lithosphere beneath the Sino-Korean Craton. In: Flower, M.F.J., Chung, S.-L., Lo, C.-H., Lee, T.-Y. (Eds.), Mantle dynamics and plate interactions in East Asia. AGU Geodynamics Series, vol. 27, pp. 107–126.

HBGMR (Hebei Bureau of Geology and Mineral Resources), 1989. Regional geology of Hebei Province. Geol. Pub. House, Beijing, pp. 1–741 (in Chinese with English abstract).

Kay, R.W., Kay, S.M., 1993. Delamination and delamination magmatism. Tectonophys 219, 177–189.

Le Maitre, R.W. (Ed.), 1989. A Classification of Igneous Rocks and Glossary of Terms. Blackwell Sci.Pub, pp. 1–31.

Liu C, 2004. Numerical simulation to tectonic and magmatic activity of North China, Ph.D.Dissertation, China Univ.Geosci.Beijing, 1–105.

Liu, G.-D., 1987. The Cenozoic rift system of the North China Plain and the deep internal process. Tectonophys. 133, 277–285.

Lu, F.-X., Zhu, Q.-W., Li, S.-T., et al., 1997. Mesozoic volcanism surrounding Songliao basin, China: implication for the relationship with evolution of basin. J. China Univ. Geosci. 8 (1), 72–77.

Menzies, M.A., Xu, Y.-G., 1998. Geodynamics of the North China Craton. In: Flower, M.F.J., Chung, S.-L., Lo, C.-H., Lee, L.-Y. (Eds.), Mantle dynamics and plate interactions in East Asia. AGU Geodynamics Series, vol. 27, pp. 155–165.

Menzies, M.A., Fan, W., Zhang, M., 1993. Paleozoic and Cenozoic lithoprobes and the loss of >120 km of Archean lithosphere, Sino-Korean craton, China. Geol. Soc. Lond. Spec. Pub. 76, 71–81.

Middlemost, E.A.K., 1994. Naming materials in the magma/igneous rock system. Earth Sci. Rev. 37.

Miyashiro, A., 1974. Volcanic rock series in island arcs and active continental margins. Am. J. Sci. 274, 321–355.

Niu, Y., 2005. Generation and evolution of basaltic magmas: some basic concepts and a new view on the origin of Mesozoic–Cenozoic basaltic volcanism in Eastern China. Geol. J. China Univ. 11 (1), 9–46.

Niu, Y., O'Hara, M.J., Pearce, J.A., 2003. Initiation of subduction zones as a consequence of lateral compositional buoyancy contrast within the lithosphere: a petrologic perspective. J. Petrol. 44, 851–866.

Remane, J., Faure-Muret, A., Odin, G.S., 2000. International stratigraphic chart. J. Stratigraphy 24, 321–340 (sup.).

Rollinsion, H., 1993. Using Geochemical Data: Evaluation, Presentation, Interpretation. Longman Group UK Ltd, pp. 1–352.

Tepper, J.H, Nelson, B.K, Bergantz, G.W., Irving, A.J., 1993. Petrology of the Chilliwack batholith, North Cascades, Washington: generation of calc-alicaline granitoids by melting of mafic lower crust with variable water fugacity. Contrib. Mineral. Petrol. 113, 333–351.

Van der Voo, R., Spakman, W., Bijwaard, H., 1999. Mesozoic subducted slabs under Siberia. Nature 397, 246–249.

Wang, R.-J., Jin, Y., 1990. Early Jurassic spilites in Beijing syncline, and their origin, western Hill, Beijing. In: Zhao, J.-S., San, W.-L. (Eds.), The geology research on western Hill of Beijing. Pub. House China Univ. Geosci., pp. 93–107 (in Chinese).

Wang, Y., Zhang, Q., 2001. Badaling granitic complex in Beijing area: their composition, geochemical characteristics and geological significance. Acta Petrol. Sin. 17, 533–540 (in Chinese with abstract).

Wang, J.-L., Li, P.-S., Zhou, D.-S., Yao, S.-C., Li, Z.-Y., 1994. Geologic characteristics of granitoids plutons and metallogenesis, Hebei Province. Geol. Pub. House, pp. 1–213 (in Chinese).

Wyllie, P.J., 1977. Crustal anatexis: an experimental review. Tectonophys 43, 41–71.

Wyllie, P.J., 1984. Constraints imposed by experimental petrology on possible and impossible magma sources and products. Philos. Trans. R. Soc. Lond. A310, 439–456.

Wilde, S.A., Zhou, X.-H., Nemchin, A.A., Sun, M., 2003. Mesozoic crust–mantle interaction beneath the North China Craton: a consequence of the dispersal of Gondwanaland and accretion of Asia. Geologia 31 (9), 817–820.

Wong, W.-H., 1927. Crustal movements and igneous activities in eastern China since Mesozoic time. Bull. Geol. Soc. China 6, 9–37.

Wu, F.-Y., Sun, D.-Y., Zhang, G.-L., Ren, X.-W., 2000. Deep geodynamics of Yanshanian movement. Geol. J. China Univ. 6 (3), 379–388 (in Chinese with English abstract).

Wu, F.-Y., Sun, D.-Y., Li, H.-M., Jahn, B.-M., Wilde, S., 2002. A-type granites in Northeastern China: age and geochemical constraints on their petrogenesis. Chem. Geol. 187, 143–173.

Xu, Y.G., 2001. Thermal-tectonic destruction of the Archean lithospheric keel beneath the Sino-Korean Craton in China: evidence, timing and mechanism. Phys. Chem. Earth, Part A Solid Earth Geod. 26, 747–757.

Xu, Y.G., Huang, X.L., Ma, J.L., et al., 2004. Crust–mantle interaction during the tectonic-thermal reactivation of the North China Craton: Constraints from SHRIMP zircon U–Pb chronology and geochemistry of Mesozoic plutons from western Shandong. Contrib. Mineral. Petrol. 147, 750–767.

Yang, G., Chai, Y.-C., Wu, Z-W., 2001. Thin-skinned thrust nappe structures in western Liaoning in the eastern sector of Yanshan orogenic belt. Acta Geol. Sin. 75 (3), 322–332 (in Chinese with English abstract).

Yogodzinski, G.M., Kay, R.W., Volynets, O.N., 1995. Magnesian andesite in the western Aleutian Komandorsky region: implications for slab melting and processes in the mantle wedge. GSA Bull. 107 (5), 505–519.

Zhang, W.Y., Zhang, K., Zhao, Y.G., et al., 1983. The Mesozoic and Cenozoic geotectonic characteristics and dynamical model of the lithosphere in North China faultblock region. Acta Geol. Sin. 57 (1), 33–42 (in Chinese, with English abstract).

Zhang, H.-F., Sun, M., Zhou, X.-H., 2002. Mesozoic lithosphere destruction beneath the North China Craton: evidence from major-, trace-element and Sr–Nd–Pb isotopic studies of FangCheng basalts. Contrib. Mineral. Petrol. 144, 241–253.

Zhang, H.F., Sun, M., Zhou, X.H., 2003. Secular evolution of the lithosphere beneath the eastern North China Craton: evidence from Mesozoic basalts and high-Mg andesites. Geochim. Cosmochim. Acta 67 (22), 4373–4387.

Zheng, J.P., Sun, M., Lu, F.X., Pearson, N., 2003. Mesozoic lower crust xenoliths and their significance in lithospheric evolution beneath the Sino-Korean Craton. Tectonophys 361, 37–60.

Zhou, X.-H., Sun, M., Zhang, G.-H., 2002. Continental crust and lithospheric mantle interaction beneath North China: isotopic evidence from granulite xenoliths in Hannuoba, Sino-Korean craton. Lithos 62, 111–124.